Journal of Controlled Release 223 (2016) 178–187

Contents lists available at ScienceDirect

Journal of Controlled Release

journal homepage: www.elsevier.com/locate/jconrel

Microneedle delivery of autoantigen for immunotherapy in type 1 diabetes

Xin Zhao [a,b], James C. Birchall [b,*], Sion A. Coulman [b], Danijela Tatovic [a], Ravinder K. Singh [a], Li Wen [c], F. Susan Wong [a], Colin M. Dayan [a], Stephanie J. Hanna [a]

[a] Diabetes Research Group, Institute for Molecular and Experimental Medicine, Cardiff University School of Medicine, Cardiff, UK
[b] School of Pharmacy and Pharmaceutical Sciences, Cardiff University, Cardiff, UK
[c] Section of Endocrinology, Yale School of Medicine, New Haven, CT, USA

ARTICLE INFO

Article history:
Received 22 December 2015
Accepted 23 December 2015
Available online 29 December 2015

Keywords:
Microneedle
Diabetes
Tolerance
Antigen presentation
Skin
Immunotherapy

ABSTRACT

Antigen specific immunotherapy mediated *via* the sustained generation of regulatory T cells arguably represents the ideal therapeutic approach to preventing beta cell destruction in type 1 diabetes. However, there is a need to enhance the efficacy of this approach to achieve disease modification in man. Previous studies suggest that prolonged expression of self-antigen in skin in a non-inflammatory context is beneficial for tolerance induction. We therefore sought to develop a dry-coated microneedle (MN) delivery system and combine it with topical steroid to minimise local inflammation and promote prolonged antigen presentation in the skin. Here we show that a combination of surface-modified MNs coated with appropriate solvent systems can deliver therapeutically relevant quantities of peptide to mouse and human skin even with hydrophobic peptides. Compared to conventional "wet" intradermal (ID) administration, "dry" peptide delivered *via* MNs was retained for longer in the skin and whilst topical hydration of the skin with vehicle or steroid accelerated loss of ID-delivered peptide from the skin, MN delivery of peptide was unaffected. Furthermore, MN delivery resulted in enhanced presentation of antigen to T cells in skin draining lymph nodes (LNs) both 3 and 10 days after administration. Repeated administration of islet antigen peptide *via* MN was effective at reducing antigen-specific T cell proliferation in the pancreatic LN, although topical steroid therapy did not enhance this. Taken together, these data show auto-antigenic peptide delivery into skin using coated MNs results in prolonged retention and enhanced antigen presentation compared to conventional ID delivery and this approach may have potential in individuals identified as being at a high risk of developing type 1 diabetes and other autoimmune diseases.

1. Introduction

Type 1 diabetes (T1D) is an autoimmune disease characterised by T-cell mediated destruction of insulin-producing beta cells in the pancreatic islets. Antigen specific immunotherapy (ASI) is the preferred approach for immunotherapy of T1D as it offers the possibility of halting beta cell destruction without systemic immunosuppression. We have previously reported the results of a phase 1A clinical trial in patients with long standing T1D, in which a proinsulin peptide, C19-A3, was administered *via* intradermal (ID) injection. This approach was shown to be safe, and in a subset of patients, increased the number of C19-A3 reactive, IL-10-producing T cells in the peripheral blood [1]. Others have also demonstrated the safety of ASI but although some protocols have showed promise they are not yet sufficiently powerful to induce tolerance [2]. Previous research in the non-obese diabetic (NOD) mouse model of diabetes has shown that tolerance to pancreatic self-antigens can be induced using peptide immunotherapy and that this effect can be enhanced through the systemic administration of glucocorticoids (GC) [3]. However, the long-term oral administration of GC is undesirable as it is associated with notable adverse effects and therefore topical GC application offers a more clinically desirable alternative.

We have previously demonstrated that even an ID injection of PBS can provoke a proinflammatory response, most likely caused by the physical trauma of the locally injected fluid bolus [4–6]. This is undesirable for the induction of tolerance. Solid microneedle (MN) delivery, in which the therapeutic antigen is "dry coated' onto the outer surface of multiple microscopic needles, potentially represents an alternative approach involving less trauma, no skin layer distension, improved antigen delivery to the dermis and epidermis and prolonged retention of the antigen in the skin. MN drug delivery devices generate less pain and irritation than conventional hypodermic needles [7–9]. Minimal skin damage also reduces microbial penetration through MN treated skin compared to conventional needles, thus reducing the risk of infection [10,11].

* Corresponding author.
E-mail address: birchalljc@cf.ac.uk (J.C. Birchall).

http://dx.doi.org/10.1016/j.jconrel.2015.12.040

In the case of dry-coated MN delivery the drug is incorporated/coated on the surface of the needle and delivery is achieved by drug diffusion from the needles and into the skin during skin insertion [12]. Such MNs have been used widely in vaccination studies to deliver inflammatory particles, for example inactivated influenza virus, virus-like particle vaccines and DNA vaccines, showing highly effective induction of local and systemic [13–16] and protective memory [17,18] immune responses. MN delivery of vaccines is able to induce stronger immune responses, compared to intramuscular or ID injection, due to improved targeting of the antigen to skin-resident dendritic cells (DCs) [19,20]. Recently, solid-coated MNs have been proposed as a more effective method of delivery to facilitate allergen immunotherapy, with authors reporting an elevated Th1 response, against the model antigen ovalbumin, compared to SC injection [21]. However, to date MN systems have not been used for the ID delivery of peptides to induce tolerance against autoimmune disease.

As well as being vaccination targets, the DCs of the epidermis and upper dermis clearly have tolerogenic potential in the resting state [22]. There may be an opportunity to promote a tolerogenic response in the DCs by optimising the environment using topically applied tolerogenic agents. For example, local treatment using GC can influence the maturation of DCs and thus promote the induction of regulatory T cells [23–26]. Short-term topical GC is well tolerated [6] however we recognise that long-term treatment may reduce Langerhans cell numbers in the epidermis [27–30].

In this project, we therefore hypothesise that delivery of auto-antigen to the upper layers of the skin using a minimally invasive MN delivery method, and a non-stimulatory coating formulation, might provide a less inflammatory and more efficient means of loading resting DCs than standard ID injection for tolerance induction. This study aims to exemplify, for the first time, the development of such a delivery system towards the future goal of preserving endogenous insulin production in type 1 diabetes. The painless nature of the delivery method and its suitability for self-administration make this a particularly attractive proposition for this patient group. Furthermore, the study also explores the potential of topical application of GC as a means to enhance any peripheral tolerance induced using MNs coated with auto-antigen.

2. Materials and methods

2.1. Reagents

All antibodies were purchased from BioLegend, eBioscience and BD. ELISAs were from R&D. Peptides were from GLS China manufactured to >95% purity with sequences as follows: BDC2.5 mimotope — YVRPLWVRME [31]; WE14 — WSRMDQLAKELTAE [32]; Epstein–Barr virus peptide (EBVP1) (lytic protein BMLF-1) (280–288)-GLCTLVAML [33], and Insulin B9-23-SHLVEALYLVCGERG.

2.2. Animal models

The BDC2.5 TCR transgenic NOD mouse expresses diabetogenic $CD4^+$ T cells that recognise the WE14 peptide from chromogranin A after it has been post-translationally modified [32]. Mice were maintained in individually-ventilated filter cages in scantainers in a specific pathogen free facility on a 12 h light/dark cycle. All procedures were performed in accordance with protocols approved by the UK Home Office.

2.3. Intradermal injection of peptide

Mice were anaesthetised using isoflurane and the site of injection was shaved using electric clippers prior to injection. Peptide was prepared in sterile PBS at a dose derived from the MN delivery efficiency studies and injected in a volume of 50 μl using a 29G insulin needle for mice and a 26G needle for human skin.

2.4. Manufacture of MNs

MNs were wire cut from stainless steel sheets using wire electrical discharge machining (wire-EDM) performed at the Cardiff School of Engineering. The MNs were subsequently electro-polished using a method adapted from that described previously [12,34]. An electrolyte bath was heated to 70 °C. The cathode was connected to a copper plate and the anode was connected to a MN array. A current of 1.8 mA/mm^2 was applied for each MN array for 15min using mechanical agitation of the MNs to remove air bubbles. After electro-polishing, the MNs were washed for 30 s in deionised (DI) water followed by 25% v/v nitric acid solution and then rinsed in hot running tap water before a final rinse in DI water. MNs were then air-dried, wrapped in lens tissue and kept in an airtight container.

A bespoke MN holder and application device was manufactured from biocompatible acrylate polymer (e-Shell 200; EnvisionTEC) at the Cardiff School of Engineering using additive manufacturing. The applicator was designed to facilitate simultaneous insertion of three planar rows of MNs.

2.5. Imaging of MNs

MNs were inspected using a stereo microscope. The surface morphology of MNs was imaged using a scanning electron microscope (SEM). All pictures were post-processed using ImageJ software.

2.6. Preparation of peptide coating formulation

BDC2.5 mimotope (with or without 5-carboxytetramethylrhodamine (5-TAMRA)) was prepared in 2.5 mg/ml polyvinyl alcohol (MW2000) (PVA 2000), 20% v/v 2-methyl-2-butanol and 11% v/v acetic acid in water. WE14 (with or without 5-TAMRA) was prepared in 2.5 mg/ml PVA 2000 and 15% v/v acetic acid. EBVP1 peptide was dissolved in 2.9 mg/ml PVA 2000, 59% v/v glacial acetic acid and 29% v/v 2-methyl-2-butanol. B9-23 was prepared in 1.25 mg/ml PVA 2000, 31.25% v/v 2-methyl-2-butanol and 12.5% v/v acetic acid in water.

To coat MNs, 0.4 μl of BDC2.5 mimotope and WE14, or 0.8 μl of B9-23 and EBVP1 formulation (containing 10 μg peptide) was taken up using a pipette and 10 μl ultra-long tip. The droplet in the tip was repeatedly applied to three rows of ten MNs resulting in a nominal coating of 10 μg peptide spread across 30 individual MNs.

2.7. Administration of peptide to mice using MNs

To apply MNs *in vivo*, the MN arrays were mounted in the applicator device, manually inserted into the shaved skin of an anaesthetised mouse and held in place for 10 min. The delivery efficiency of 5-TAMRA conjugated peptides was calculated by measuring the mass of peptide remaining on the MN device following insertion. To determine the remaining peptide the MNs were washed in 10% v/v acetic acid and the resulting solution of peptide was quantified using UV–vis spectrometry at the maximum absorption wavelength of 559 nm (as identified from a wavelength scan between 200 nm and 800 nm; Nanovue®). The delivery efficiency of peptides was then calculated using the equation below:

$$\%\text{delivered} = (\text{mass before delivery} - \text{mass post delivery})/(\text{mass before delivery}) \times 100.$$

The same UV–vis quantification method was also used in delivery efficiency experiments performed in excised human skin. Fluorescence quantification was not employed due to the inherent autofluorescence that is associated with mouse and human skin.

2.8. Application of GC cream

In steroid pre-treatment studies a 0.1 ml volume of cream was applied to the shaved back of the neck and gently massaged into the skin. To study the systemic effect of betamethasone, DiproSone® 0.05% w/w Cream (0.05% w/w betamethasone dipropionate; Schering Plough) was used either in its original form or following a 1/50 (0.001% w/w) dilution in Diprobase Cream (geometric dilution on a ceramic tile).

2.9. Flow cytometry

Flow cytometric analysis was performed on a BD Canto II with data analysed by FlowJo. Cells were gated on singlet cells, and dead cells were excluded using a fixable viability dye (eBioscience).

2.10. In vivo imaging of peptide distribution in murine skin

NOD mice (5–7 weeks old) were shaved in the neck area under general anaesthetic. Mice were imaged before and after peptide delivery (via ID injection and MN array) using a Kodak Fx Pro *in vivo* imaging system. Images were analysed using Carestream MI software. For each fluorescent image, the same area of the region of interest (ROI) was applied to all the data. Net intensity for the ROI was calculated by subtracting net intensity of the skin prior to treatment from the values obtained from the treated area. The normalised relative intensity (NRI) was calculated using the following equation:

$$\mathrm{NRI}(\%\,\mathrm{max}) = (\text{Net intensity at each time point}/\text{Maximum net intensity}) \times 100.$$

Mice were imaged before treatment and then 1, 4 and 24 h post treatment. Between each time point, the mouse cage was maintained at 26 ± 1 °C.

2.11. CFSE-labelled cell transfer

$CD4^+$ T cells were separated from splenocytes using a MACS CD4 II isolation kit from Miltenyi Biotec. Cells were labelled with 20 μM CFDA (Invitrogen) in 10% FCS RPMI at room temperature for 5 min at a concentration of 10^7/ml. Cells were then washed twice in RPMI containing 10% foetal calf serum (FCS) and rested for 15 min in the same media. Cells were subsequently washed in saline, re-suspended at 4×10^6 cells in 200 μl sterile saline and injected into a tail vein using a 27G needle.

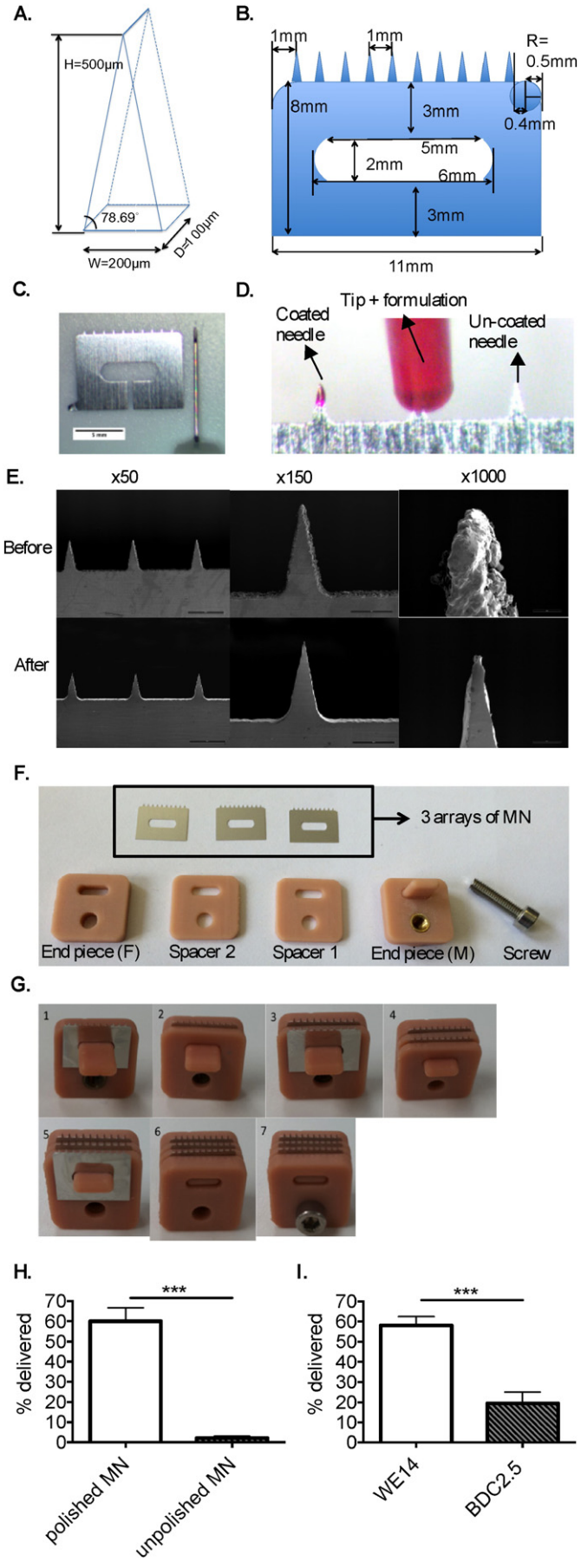

Fig. 1. Design of MNs suitable for both human and mouse studies. A. Individual needle dimensions (μm): 500 (L) × 200 (W) × 100 (D); B. MN array design. Each MN array contains 10 needles (A) spaced 1 mm apart. A channel was designed in the centre of each MN array so that MNs can be held together using a bespoke MN holder (F & G); C. A single stainless steel MN array (left) shown with a 29G insulin injection needle for scale (right); D. Coating technique; Each needle was manually coated with peptide using a fine pipette tip, filled with 10 μg peptide (pink); E. Scanning electron microscopy (SEM) image of a MN tip before and after electropolishing; F. The elements contained in each MN set; the 3 MN arrays are held in place between the end plates and are separated by spacers; G. Sequential assembly of a MN set. MN arrays are located on the male end piece as shown (1, 3 and 5), each followed by a spacer (2 and 4). The female end piece completes the assembly (6), which is then carefully tightened and secured with a screw (7); H. MNs with and without electropolishing were coated with 10 μg BDC2.5-5TAMRA mimotope peptide and applied to mouse skin for 10 min. The remaining peptide was dissolved off the MN and analysed by UV–vis spectrophotometric analysis to calculate the % delivered to skin (***$p < 0.001$ unpaired t test n = 3, Mean ± SD); I. Polished MNs were coated with 10 μg of either BDC2.5-5TAMRA or WE14-5TAMRA and the amount delivered to the skin was quantified as above (***$p < 0.001$ unpaired t test n = 3–11, Mean ± SD).

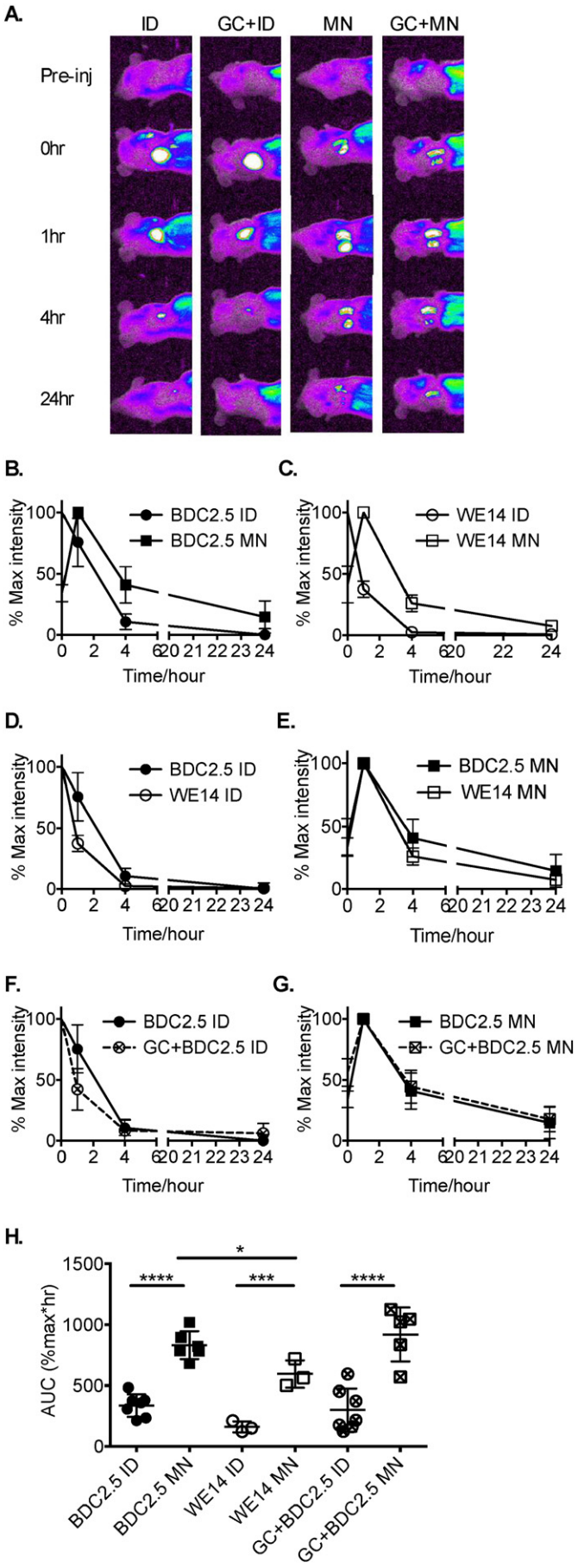

Fig. 2. MN delivery improves skin retention of peptide *vs.* ID injection. Mice were injected with 2 μg BDC2.5-5TAMRA unless otherwise stated, using conventional ID or coated-MN injection. A. The total fluorescence was measured before and immediately after injection and again 1, 4 and 24 h post injection using a Kodak *in vivo* imaging system (BDC2.5-5TAMRA). Images presented are from a single experiment representative of at least 3 independent experiments; B. The percentage of the maximum fluorescence at each timepoint was calculated in for BDC2.5-5TAMRA delivered by ID or MN (n = 6); C. The percentage of the maximum fluorescence at each timepoint was calculated for each mouse for WE14-5TAMRA delivered by ID or MN (n = 3); D. Comparison of ID injection of BDC2.5-5TAMRA and WE14-5TAMRA; E. Comparison of MN injection of BDC2.5-5TAMRA and WE14-5TAMRA; F. Mice were pretreated with GC cream for 2 days before ID injection of BDC2.5-5TAMRA; G. Mice were pretreated with GC cream for 2 days before MN injection of BDC2.5-5TAMRA (n = 7). H. The AUC of maximum fluorescence *vs.* time was calculated for each mouseover the 24 h period (*$p < 0.05$, ***$p < 0.001$, ****$p < 0.0001$ One way ANOVA with Tukey's post test, Mean ± SD). AUC = area under curve.

2.12. Peptide delivery to ex vivo human skin

Skin samples were obtained from female patients aged 19–82 years, following mastectomy or breast reduction after informed consent. Skin without obvious pathological findings, that was surplus to diagnostic histopathology requirements, was used in the experiments. The study received full ethical approval from South East Wales Research Ethics Committee, UK.

Subcutaneous adipose tissue was removed by blunt dissection to yield full-thickness skin. EBVP1 was coated on MNs, which were then applied to *ex vivo* human skin and kept *in situ* for 15 min. Skin samples were also treated with MNs coated with vehicle only (negative control) or by ID injection of 2 μg (equivalent to MN delivery amount) of peptide in 50 μl of PBS using a 26G hypodermic needle.

Treated skin was isolated as previously described [6] using a disposable 0.8 cm biopsy punch and punches were then cultured at the air-liquid interface using cell culture inserts and DMEM media supplemented with 50 IU/ml penicillin and 50 μg/ml streptomycin at 37 °C in 5% (v/v) CO_2/95% (v/v) air for 16–18 h [35]. After incubation, a single cell suspension was obtained and co-cultured with HLA-A*0201 (HLA-A2) restricted EBVP specific cloned T cells for 12 h. Supernatants were harvested for Macrophage Inflammatory Protein 1β (MIP-1β) measurements by ELISA (human CCLR/MIP-1β, DuoSet® Development System, R&D Systems, Abingdon, UK).

2.13. Statistical analysis

Data are expressed as mean ± SD. Statistical significance of differences was determined using unpaired t tests or one-way ANOVA, followed by appropriate post hoc tests. P-values are expressed in the figure legends. Statistical analysis was performed using GraphPad Prism software.

3. Results

3.1. Coated MNs for the delivery of peptides into murine skin

Solid MNs with dimensions of 500 μm (L) × 200 μm (W) (Fig. 1A) were prepared by wire electro-discharge machining (EDM) of 100 μm thick stainless steel sheets. The MNs were composed of 10 in-plane needles, each 1 mm apart (Fig. 1B). In this study MN delivery was compared to standard ID injection using a 29G insulin needle (Fig. 1C). MNs were coated with various peptides using a simple yet reproducible pipette tip method (Fig. 1D) [36]. Needles were left unpolished or deburred and sharpened by electropolishing prior to coating (Fig. 1E). The polishing process reduced the length of the MN by approximately 50 μm, to give a length of approximately 450 μm. Electropolishing the MNs prior to coating increased the efficiency of delivery of peptides into murine skin, with 60% of the WE14-TAMRA peptide delivered to skin when coated onto 30 electropolished needles versus 2% delivery from unpolished MNs (Fig. 1H). Therefore all further experiments

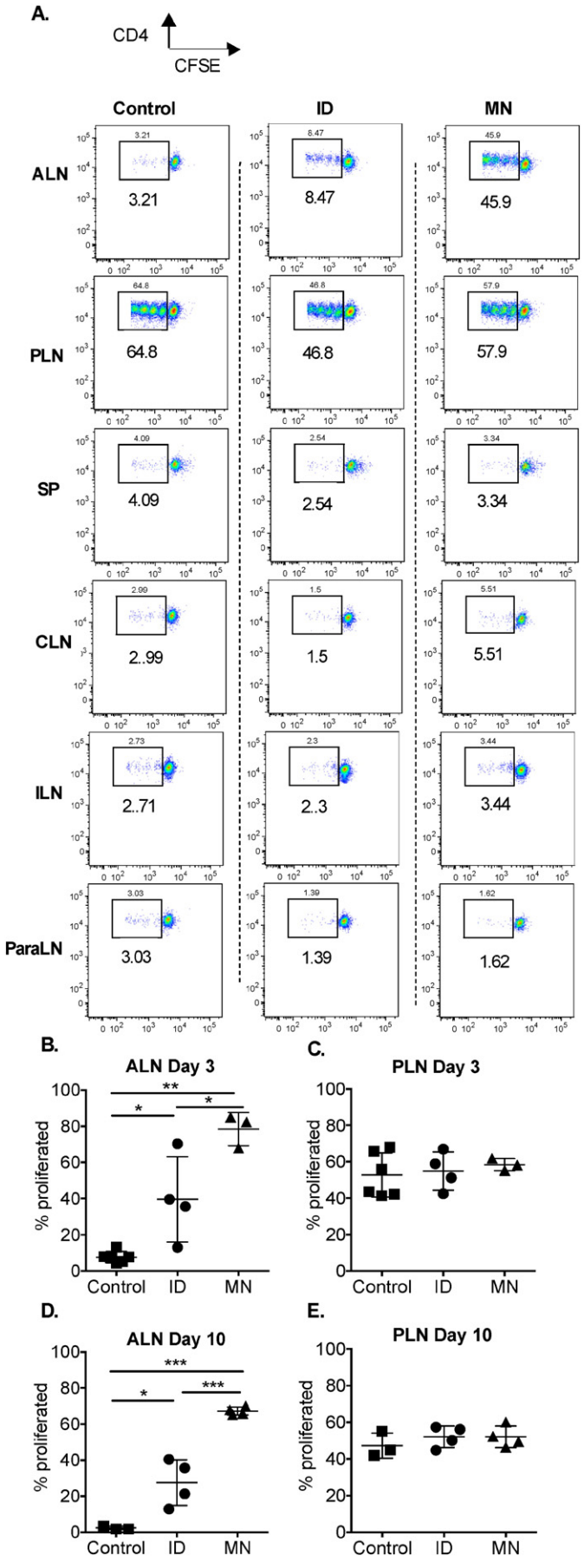

used electropolished MNs. Three arrays of MNs were assembled into a biocompatible polymer applicator device (Fig. 1F and G) to enable 30 MNs to be administered in a single application. We then compared delivery between peptides of different composition. When 10 μg of either BDC2.5 mimotope peptide conjugated to the fluorescent TAMRA tag (BDC2.5-5TAMRA) or WE14-5TAMRA (WE14 is more hydrophilic than BDC2.5 mimotope) was coated onto 30 MNs we found that 19.5% *vs.* 58.2% of coated BDC2.5 mimotope or WE14 peptide, respectively, was delivered to skin (Fig. 1I). Hence in further experiments, whilst 10 μg of peptide was coated onto all solid MN, the dose of peptide delivered into skin was considered to be 2 μg for BDC2.5 mimotope and 6 μg of WE14, and equivalent doses were therefore also delivered by ID injection for the ID controls.

3.2. Comparison of pharmacokinetics of ID and MN delivery of peptide

Fluorescently-tagged peptides and the Kodak intravital imaging system were used to monitor peptide retention in the skin following delivery (Fig. 2A). In order to standardise experiments and peptides, the fluorescence was calculated as a percentage of maximum fluorescence for each mouse. Fluorescence of BDC2.5-5TAMRA injected ID fell by 25% at 1 h and declined to near baseline by 4 h. However, MN-injected peptide intensity increased over the first hour (the TAMRA tag only fluoresces in solution) and then declined slowly, with ~45% of the maximum fluorescence remaining at the 4 h time-point, before decreasing to comparable levels to ID injection at 24 h (Fig. 2B). The signal from the peptide with higher solubility, WE14-5TAMRA, followed the same general trend (Fig. 2C) however side by side comparisons (Fig. 2D and E) of the clearance kinetics of the two peptides reveal some subtle differences. For example, when administered by ID injection, the fluorescent signal of WE 14-5TAMRA dropped sharply within 1 h compared with BDC2.5-TAMRA. At the 4 h timepoint, WE14-5TAMRA was almost entirely eliminated from the skin, whilst BDC2.5-TAMRA was still traceable (Fig. 2D). Using MN delivery, both WE14-5TAMRA and BDC2.5-TAMRA showed similar skin clearance kinetics within the first hr. However, WE14-5TAMRA was cleared more quickly from the skin from 1 h onwards (Fig. 2E).

As ID application of peptides for ASI offers the opportunity of modulating local DCs to improve tolerance induction without systemic side effects, we also pre-treated the skin with GC cream for two days prior to peptide application. The clearance of BDC2.5-TAMRA was initially, *i.e.* within the first hr, twice as rapid following ID administration in mice pretreated with GC cream (40% of maximum intensity compared with 80% in non-GC treated mice) (Fig. 2F). However, when MNs were used to administer BDC2.5-TAMRA there was no statistically significant difference in peptide signal in the skin at 1, 4 and 24 h in steroid pretreated and non-treated mice, although the initial signal (immediately after injection) was slightly higher in GC-treated mice (60% compared with 40%) presumably due to enhanced solubility of the peptide in the more hydrated skin (Fig. 2G). To investigate whether the altered effect on pharmacokinetics after ID administration to GC-treated skin could have been due to a deleterious effect of GC on skin integrity [37], we reduced the time that GC cream was applied to as little as 1 h before peptide injection and found that this or a placebo vehicle cream also caused a reduction in peptide retention (Supplementary Fig. 1).

Fig. 3. Proliferation of transferred BDC2.5 T cells following topical peptide administration. A. Female NOD mice were given 2 μg BDC2.5 mimotope peptide by ID injection or coated MNs and 4×10^6 CFSE-labelled BDC2.5 $CD4^+$ T cells were transferred. CFSE dilution was assessed after 72 h. Representative flow cytometry plots from pancreatic lymph node (PLN), axillary LN (ALN), spleen (SP), cervical LN (CLN), inguinal LN (ILN) and paraaortic LN (ParaLN) from one experiment representative of two independent experiments are shown. B. Graph summarizing proliferation in axillary LN (ALN) at 3 days post treatment (*$p < 0.05$ **$p < 0.01$ one way ANOVA followed by Bonferroni post test); C. Graph summarizing proliferation in pancreatic LN (PLN) at 3 days; D. Proliferation in ALN at 10 days (**$p < 0.01$ ***$p < 0.001$ one way ANOVA followed by Bonferroni post test); E. Proliferation in PLN at 10 days. All data are presented as Mean ± SD.

In addition to displaying the kinetic profiles we also calculated the total AUC of % maximum fluorescence *vs.* time for the 24 h experimental period (Fig. 2H). AUC is inversely correlated with the clearance rate, therefore the higher the AUC the lower the clearance rate. The AUC for BDC2.5-TAMRA peptide administered *via* coated MNs (832.6 ± 115.1) was significantly higher than for peptide administered via ID injection (336.7 ± 92.99) confirming a slower skin clearance rate for MN delivered peptide. There was also a significant increase in AUC when WE14-TAMRA was given by MN (595.5 ± 111.6) rather than ID injection (162 ± 45.54). Looking at the above data therefore, peptide solubility was confirmed to play a role in clearance with MN delivery of BDC2.5-5TAMRA showing a significantly higher AUC than the relatively more soluble WE14-5TAMRA. Despite the aforementioned observation of an initial increase in clearance of BDC2.5 peptide administered via ID injection following skin pre-treatment with GC cream the AUC over 24 h was not significantly affected (300.2 ± 177.2 for steroid pre-treated skin *vs.* 336.7 ± 92.99 for non-treated skin).

3.3. Antigen presentation in draining LN following ID and MN peptide administration

To determine if the apparently longer retention of peptide in skin following MN delivery results in greater peptide delivery to the draining LN, we explored the potential of MN versus ID peptide to stimulate T cells. Following transfer of islet-specific BDC2.5 T cells into an untreated NOD mouse, the T cells proliferated at the site where they encountered their cognate antigen *i.e.* in the pancreatic LN (PLN) (~50% of cells proliferated), as well as undergoing a low level of proliferation in the spleen and other LNs (<5%). This was observable at 72 h post transfer (Fig. 3A). The high affinity BDC2.5 mimotope peptide was administered into the skin of the back of the neck (at the same time as the BDC2.5 T cells were transferred). After 72 h, the BDC2.5 T cells were observed to proliferate in the skin-draining (axillary) LN (ALN) as well as the PLN, but not in non-draining LNs (cervical (CLN) or inguinal (ILN)) (Fig. 3A). MN administration of peptide resulted in a higher and more consistent level of proliferation in the skin-draining LN compared to ID injection (78% ± 9 SEM MN *vs.* 39.6% ±23.6 ID) (Fig. 3B). ID or MN-administered peptide had no effect on proliferation in the PLN at this early time point (Fig. 3C). To test for prolonged antigen retention in skin and delivery to draining LN, we repeated the experiment with cells transferred into mice 7 days after a single treatment with peptide, and examined proliferation at day 10 in the ALN. The response to MN-delivered peptide continued to be greater than to ID peptide, with less variability (MN 67.25 ± 2.2 SEM *vs.* ID 27.58 ± 12.8) (Fig. 3D). Again, no changes in the level of proliferation in the PLN were observed (Fig. 3E).

3.4. Delivery of peptide into ex vivo human skin

Human skin is architecturally very different from mouse skin, with a 10-fold thicker epidermis, a dermis that is millimetres thick and more subcutaneous tissue. We therefore sought to determine the ability of MNs to effectively deliver peptide to human skin. MNs of 500 μm length, coated with 10 μg of EBVP1, were inserted into human skin explants and kept in place for 15 min. Spectrophotometric analysis of the EBVP5-TAMRA, which, like BDC2.5 mimotope, is another poorly-soluble peptide, remaining on the MNs indicated that 17.0 ± 1.4% of the coated peptide was deposited in the skin (Fig. 4A). We also examined the delivery efficiency of Insulin B9-23 and WE14 peptides to human skin explants which were found to be 46.5% and 81.4% respectively (Fig. 4A). The delivery efficiency of WE14 was compared between human skin explant and mouse skin (Fig. 4B). Significantly more peptide was delivered to human skin (81.4 ± 2.6% *vs.* 58.2 ± 4.2%).

To study delivery of antigen to local DCs in human skin, the EBVP1 peptide was delivered to human skin explants that were then maintained in organ culture. After 16–18 h, the skin epithelial cells (ECs) were harvested to make a single cell suspension and incubated with an EBVP1-specific T cell clone. The response measured by MIP-1β production (expressed as a ratio of peptide treated/non treated cultures) showed significant increases in MIP-1β production when peptide was delivered by MNs (Fig. 4C) in HLA-A2 positive donors versus HLA-A2 negative donors. MIP-1β production was not significantly increased when peptide was administered by ID injection. Presentation was shown to be specific, as no response was seen with ECs from donors that did not carry the MHC-restriction element (HLA-A2) for this peptide (Fig. 4C). It is however not possible to examine the time course of peptide retention using such *ex vivo* systems.

3.5. Downregulation of the in vivo response to endogenous pancreatic antigen following administration of peptide by MN versus ID injection

To attempt to induce immune tolerance by auto-antigenic peptide administration, we administered two doses of peptide, three weeks apart, by either MN or ID injection, to female NOD mice. CFSE-labelled BDC2.5 T cells were then adoptively transferred and we assessed proliferation in response to endogenous antigen presentation in the PLN

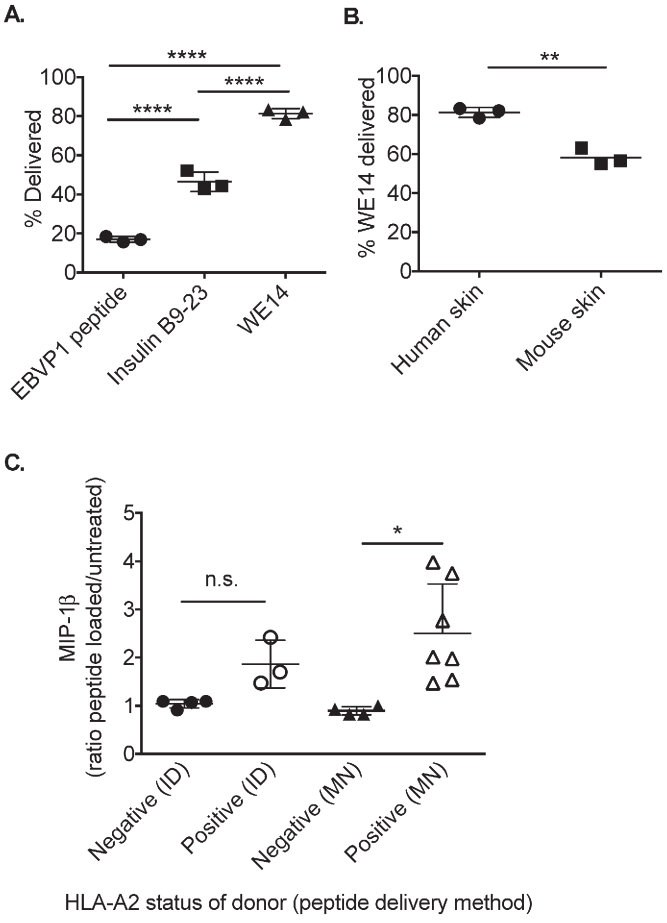

Fig. 4. Peptide delivered to human skin explants using MNs is presented to T cell clones. A. EBVP1 peptide, Insulin B9-23 and WE14 were coated onto arrays of MNs and the MNs were applied to human skin explants. The remaining peptide was dissolved off the MN and analysed by UV–vis spectrophotometric analysis to calculate the % delivered to skin (****$p < 0.0001$, One way ANOVA followed by Bonferroni post-test); B. MNs were coated with 10 μg WE14 and applied to human skin explant or mouse skin. The percentage delivered was calculated by UV–vis spectrophotometric analysis (**$p < 0.01$, unpaired t test). C. EBVP1 peptide (2 μg) was delivered to human skin explants from HLA-A2 negative or positive donors by standard 26G needle (ID) or dry coated MNs. The epithelium was mechanically and enzymatically digested to a single cell suspension and used to present peptide to the T cell clone. MIP-1β produced by the T cells was measured and expressed as a ratio of peptide treated/untreated controls (*$p < 0.05$, One way ANOVA followed by Bonferroni post-test). All data are presented as Mean ± SD.

(Fig. 5A). BDC2.5 mimotope peptide, which is of very high affinity for islet infiltrating T cells, did not induce tolerance in this protocol (Fig. 5B). Although low-dose administration of 6 μg of the low-affinity WE14 peptide did not induce a significant decrease in proliferation of the transferred T cells in the PLN when administered ID, there was a significant decrease in proliferation when this dose of WE14 was administered using MNs. A much higher dose of 50 μg of WE14 was required to achieve a significant response reduction using the ID route (Control 50.4% ± 1.3, ID 6 μg 42.7 ± 2.8 MN 6 μg 36.5 ± 3.4, ID 50 μg 28.5 ± 3.3) (Fig. 5C).

3.6. The effect of topical GC on tolerance induction

We sought to further optimise tolerance induction by pre-treatment with topical glucocorticoid (GC) cream. GC cream did not however improve tolerance with BDC2.5 mimotope or WE14 peptides, despite efforts to titrate the dose to limit systemic side effects (Fig. 6).

4. Discussion

We have developed a protocol that uses non-inflammatory formulations to coat soluble and insoluble peptides onto electropolished steel

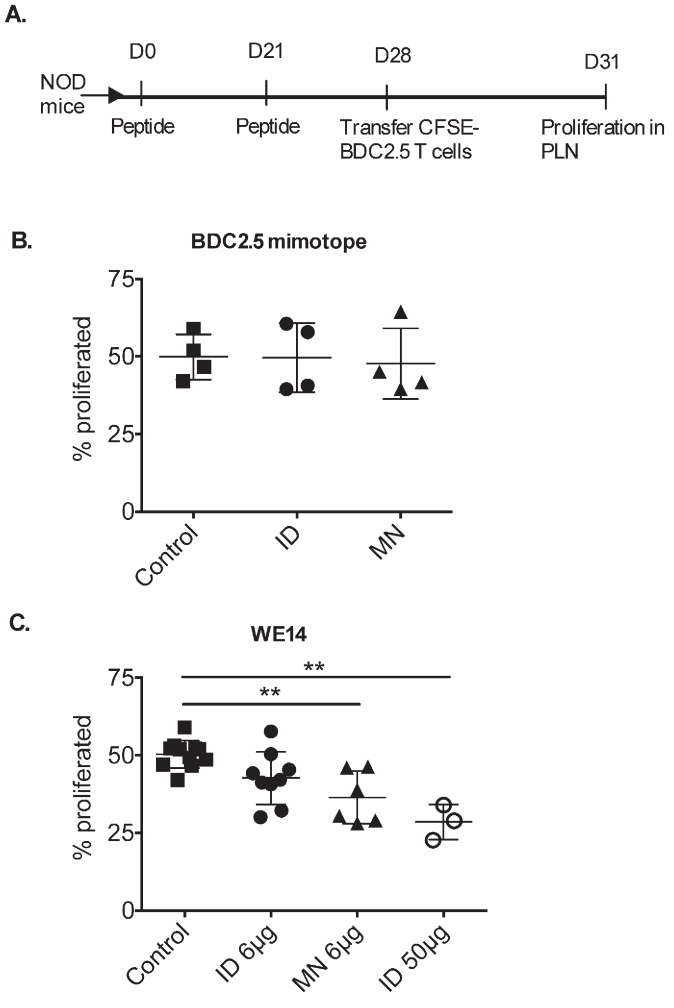

Fig. 5. Tolerisation followed by transfer of CFSE-labelled BDC2.5 T cells: A. Mice were given 2 doses of BDC2.5 mimotope peptide (B) or WE14 peptide (C), 3 weeks apart by MN or ID injection. CFSE-labelled BDC2.5 T cells were transferred 7 days after the last injection and mice were examined after 72 h and the presence of proliferated BDC2.5 T cells was assessed in LNs and spleen. B. After administration of 2 μg BDC2.5 mimotope peptide: % $CFSE^+$ cells proliferated in PLN. C. After administration of WE14 peptide: % $CFSE^+$ cells proliferated in PLN (**$p < 0.01$ one way ANOVA followed by Dunnett's post test). All data are presented as Mean ± SD.

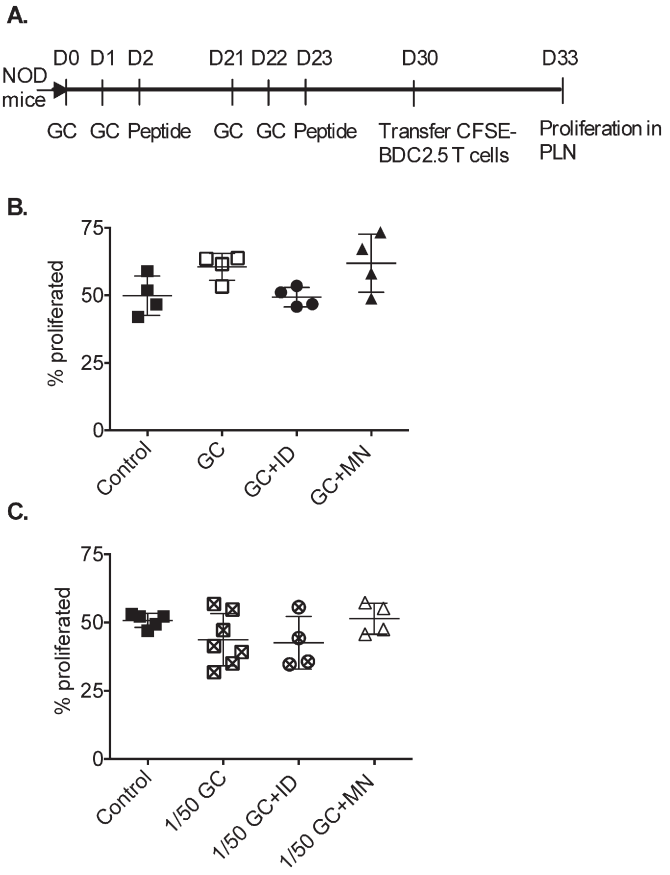

Fig. 6. Tolerisation followed by transfer of CFSE labelled BDC2.5 T cells: A. Mice were given 2 doses of peptide 3 weeks apart by MN or ID injection. Before each dose of peptide mice were pre-treated with GC (B) or GC diluted 1/50 in vehicle cream (C). CFSE-labelled BDC2.5 T cells were transferred 7 days after the last injection and mice were culled after 72 h and the presence of proliferated BDC2.5 T cells was assessed in LNs as shown in the schematic. B. Graph illustrating proliferation of BDC2.5 T cells after 2 μg BDC2.5 mimotope peptide with or without GC cream. C. Graph illustrating proliferation of BDC2.5 T cells after 6 μg WE14 peptide with or without 1/50 GC cream. All data presented as Mean ± SD.

MNs that can deliver significant quantities of peptides into mouse and human skin. Here we show that MN-delivered peptide is retained in the skin for longer and results in greater delivery to the immune system than fluid-phase peptide administered by standard ID hollow needle injection. When we administered low affinity peptide as two separate injections over a 21 day period, the peptide coated onto MNs was more efficient at reducing the response to self-antigen in the pancreas in the NOD mouse model of diabetes than the same dose of peptide in fluid phase (ID), suggesting that this approach may be beneficial for tolerance induction. Peptide delivered in solid phase, using coated MNs, was also better retained in the skin than ID injection of fluid phase peptide following pre-treatment with topical GC cream. However, in the protocols used, topical GC therapy abrogated rather than enhanced tolerance induction for both methods of delivery and therefore may not be required in the clinical protocol.

The delivery of peptide into skin using coated MNs is predominantly determined by the detachment of the peptide from MN surface and peptide dissolution in skin. The efficiency of the first process is related to MN surface morphology. The reduction of MN surface roughness, by electropolishing, minimised the retention of the coated material to the needle surface, which enabled efficient delivery of MN load upon skin insertion. The efficiency of the second process is related to factors such as peptide solubility, formulation excipients, the thickness of the coating and the skin condition [34]. The combined effect of these two processes determines the final delivery dose of coated peptide. The

restricted water content of the skin limits the amount of peptide that can be dissolved during the insertion period. This limitation is particularly problematic when coating peptides of increased hydrophobicity, such as the BDC2.5 mimotope peptide; nevertheless we were able to consistently and reproducibly deliver the coated peptide into the skin. MN delivery of the WE14 peptide is more efficient than the BDC2.5 mimotope, in line with its increased solubility. The BDC2.5 mimotope peptide was also retained for longer in the skin than WE14, which again reflects their respective solubilities.

It is well known that there are a variety of tolerogenic APCs in the skin, which take up antigen *in situ* and then migrate to the draining LN to exert tolerogenic effects [38,39]. However, ID-delivered peptides can also move in a fluid phase to the draining LN to be presented by resident DCs [40,41]. Skin DCs are able to take up peptide between 40 and 360 min post treatment [42] and appear in the draining LNs just 24 h after exposure to antigen [43]. Our data tracking fluorescently-labelled peptide suggests that most peptide is cleared from the skin in mice within 4 h post ID injection, which limits the time available for antigen uptake by APCs in the skin.

We demonstrated that MN application led to prolonged retention of peptide in the skin compared to ID injection, which would be expected to facilitate uptake by APCs in the skin and hence to favour tolerance induction. Prolonged exposure to antigen is beneficial to tolerance induction [44]; therefore the more sustained presentation in the draining LN observed when peptide was administered by MN is also likely to be relevant to tolerance induction. Others have shown that dose escalation protocols can induce tolerance [45], and this relies upon accurate delivery of known doses. We hypothesise that the highly reproducible cellular response to MN-delivered peptide would make MNs delivery ideal for these procedures. Importantly, this study has also demonstrated that peptide coated onto solid MNs using our non-inflammatory solvents, can be delivered into human skin and functionally presented by dermal APCs to T cells.

MNs have been shown to reduce trauma at the injection site [46]. This is essential for a protocol aimed at inducing tolerance, as any inflammation at the injection site may lead to activation of Langerhans cells and dermal DCs and could result in a sensitisation response to the peptide [47]. Solid MNs have previously been used to deliver peptides and vaccines; however these are often coated with immunogenic coating formulations. In order to reduce immunogenicity we therefore coated our MNs by dissolving the peptide in a solution of PVA. PVA 2000 is known to be a useful excipient for *in vivo* and *in vitro* medical applications due to its documented stability, biocompatibility and low toxicity [48]. ID injection delivers the peptide to the lower dermis, whereas MNs administer peptide more superficially and are able to target the epidermis and papillary dermis (as result of the dip-coating procedure used to apply peptide). This may be advantageous for tolerogenic protocols as others have shown that Langerhans cells (which reside in the epidermis) in particular can be excellent mediators of tolerance [39]. Using the reduced proliferation of transferred BDC2.5 T cells to endogenous pancreatic antigen in the NOD as an established surrogate measure of tolerance induction [49], we were able to show that MN administration of WE14 did indeed show tolerogenic potential. Whilst we found that both ID and MN delivery of WE14 could reduce proliferation of transferred BDC2.5 cells to native antigen, MN delivery required less peptide to achieve the effect, in line with reports that MNs provide a dose sparing effect for vaccination applications [50].

Others have hypothesised that high affinity mimotopes are better than native peptides at inducing tolerance as they are more efficient at converting naïve T cells into Tregs [51]. However, our studies suggest the opposite to be the case, with the native low-affinity WE14 peptide and not the high-affinity mimotope able to reduce proliferation of transferred cells. This is also in line with the finding that tolerising peptides should ideally be both highly soluble and contain a native peptide sequence [52].

GC cream topical pre-treatment increased clearance of peptide from the skin following ID injection. This appeared to be *via* increasing the hydration of the treated skin tissue as a placebo vehicle cream had similar effects (Supplementary Fig. 1). MN administration abrogated the negative impact of GC or vehicle cream pre-treatment on peptide retention compared to ID injection. As previously discussed, we believe that it is undesirable for peptide to be rapidly lost from the skin in ASI [38,41] and therefore MNs are likely to be better suited than ID injection for peptide administration in conjunction with other topical pre-treatments that may hydrate the underlying skin tissue.

Others have shown that systemic GC can enhance tolerance [24], however it can also cause systemic immunosuppression [3]. We therefore used topical GC pre-treatment in an effort to enhance tolerance induction whilst minimising systemic exposure and side effects. However, in the protocol used, topical GC inhibited rather than augmented tolerance induction. We hypothesise that in our murine system local cell death caused by topical steroid [53] is exacerbated by the thinner murine epidermis and results in a less tolerogenic environment in the skin draining LN. This effect may be reduced in human skin (which is substantially thicker [6], Supplementary Fig. 2) and we have recently demonstrated that topical GC in humans promotes a tolerogenic phenotype in epidermal DCs [6]. In addition, alternative topical treatments such as 1,25 dihydroxy-Vitamin D_3 may have a net enhancing effect in tolerance protocols when applied to human skin [49].

Previous studies have shown that epicutaneous antigen administration can be tolerogenic in the context of allergies [54,55] and autoimmune disease [56,57]. These reported epicutaneous tolerance protocols have exploited skin barrier disruption technologies including transdermal patches, laser poration and tape stripping. Clinical studies have shown that both food allergens, *e.g.* cow's milk and peanut [58,59], and environmental allergens, such as pollen [59,60], delivered epicutaneously, *i.e.* superficially into the skin, can induce a protective response, although epicutaneous delivery of exogenous antigen has also shown to reverse the tolerance induced by oral delivery [61]. Both allergies and autoimmune diseases can be classified as hyper-immune response conditions, therefore tolerance protocols from allergy treatments have been adopted and adapted for autoimmune disease. There are, however, fundamental differences between these two immune dysfunctions. Allergies are triggered by transient exposure to one or more *exogenous* antigens whilst autoimmunity results from constant exposure to one or more *endogenous* antigens. Allergy is a Th2 mediated immune response whilst T1D is a Th1 mediated immune response. The causal factors are well characterised and identifiable with allergies and allergen testing and therapies tend to be more effective. In the case of autoimmune disease, there are usually a number of different antigens involved and identification of a single causal antigen is more difficult. Therefore, overall, the majority of the more clinically advanced tolerance protocols using epicutaneous administration are targeted at reducing allergic (Th2-driven) responses, rather than tolerising to prevent autoimmunity (primarily Th1 driven). It should also be noted that the autoimmune disease, Experimental Autoimmune Encephalomyelitis (EAE), reported in the cited studies using epicutaneous antigen administration [56,57] is an induced autoimmune disease, produced with defined antigens or peptides. The autoimmune diabetes that we study, by contrast, occurs spontaneously in our model and therefore, the application of epicutaneous therapy, consistency and timing is much more problematical. We have previously studied epicutaneous administration of antigen and this failed to induce tolerance in diabetes (data not shown).

MNs have been widely used in the context of vaccine delivery [13–16] and the induction of a pro-inflammatory response. More recently they have also been reported to be able to increase Th1 response against ovalbumin as a model allergen [21]. Our study demonstrates, for the first time, that MNs have potential utility for the delivery of endogenous, low affinity auto-antigens into human and mouse skin for the induction

of tolerance in an autoimmune condition, T1D. Importantly, delivery of the auto-antigen using coated MNs was more effective than ID injection as a result of improved targeting to the superficial skin layers, increased residence time in the skin and more efficient and persistent trafficking of the peptide to the lymph nodes. Auto-immune therapy is likely to require chronic administration of the auto-antigen and therefore the reduced pain associated with MNs and their potential for self-administration will also offer significant practical benefits to those at-risk individuals who may require preventative therapy for the duration of their life.

The method of delivery of WE14 using peptide-coated MNs is potentially translatable to humans as WE14 has recently been identified as an antigen in human type 1 diabetes [62]. The technique also has the potential to work with other known peptide auto-antigens such as insulin B9-23 [63–65] and proinsulin C19-A3 [1,66], whole small proteins such as proinsulin, as well as in other autoimmune diseases in which antigen specific therapy has been developed [67]. Taken together with the ease of self-administration and reduced discomfort of solid MNs as compared to conventional ID administration, this approach may be particularly suited to use in children and in "prevention" protocols for use in individuals identified as being at a high risk of developing autoimmune disease [68,69].

Acknowledgements

Cloned T cells were a kind gift of Dr. A. Godkin and Prof. A. Sewell (Cardiff University). This work was funded by the NAIMIT project in the 7th Framework Programme of the European Community, Juvenile Diabetes Research Foundation, and Novo Nordisk UK Research Foundation.

Appendix A. Supplementary data

Supplementary data to this article can be found online at http://dx.doi.org/10.1016/j.jconrel.2015.12.040.

References

[1] S.L. Thrower, L. James, W. Hall, K.M. Green, S. Arif, J.S. Allen, C. Van-Krinks, B. Lozanoska-Ochser, L. Marquesini, S. Brown, F.S. Wong, C.M. Dayan, M. Peakman, Proinsulin peptide immunotherapy in type 1 diabetes: report of a first-in-man phase I safety study, Clin. Exp. Immunol. 155 (2009) 156–165.
[2] K.C. Herold, D.A.A. Vignali, A. Cooke, J.A. Bluestone, Type 1 diabetes: translating mechanistic observations into effective clinical outcomes, Nat. Rev. Immunol. 13 (2013) 243–256.
[3] Y. Kang, L. Xu, B. Wang, A. Chen, G. Zheng, Cutting edge: immunosuppressant as adjuvant for tolerogenic immunization, J. Immunol. 180 (2008) 5172–5176.
[4] T. Eberle, B. Doganci, H. Krämer, M. Fechir, I. Wagner, C. Sommer, F. Birklein, Mechanical but not painful electrical stimuli trigger TNF alpha release in human skin, Exp. Neurol. 221 (2010) 246–250.
[5] L. Liu, X. Zhou, J. Shi, X. Xie, Z. Yuan, Toll-like receptor-9 induced by physical trauma mediates release of cytokines following exposure to CpG motif in mouse skin, Immunology 110 (2003) 341–347.
[6] M. Alhadjali, S.L. Thrower, S.J. Hanna, S. Coulman, J.C. Birchall, F.S. Wong, C.M. Dayan, D. Tatovic, Topical steroid therapy induces pro-tolerogenic changes in Langerhans cells in human skin, Immunology (2015).
[7] S.M. Bal, J. Caussin, S. Pavel, J.A. Bouwstra, In vivo assessment of safety of microneedle arrays in human skin, Eur. J. Pharm. Sci. 35 (2008) 193–202.
[8] J. Gupta, H.S. Gill, S.N. Andrews, M.R. Prausnitz, Kinetics of skin resealing after insertion of microneedles in human subjects, J. Control. Release 154 (2011) 148–155.
[9] S. Kaushik, A.H. Hord, D.D. Denson, D.V. McAllister, S. Smitra, M.G. Allen, M.R. Prausnitz, Lack of pain associated with microfabricated microneedles, Anesth. Analg. 92 (2001) 502–504.
[10] R.F. Donnelly, T.R. Singh, M.M. Tunney, D.I. Morrow, P.A. McCarron, C. O'Mahony, A.D. Woolfson, Microneedle arrays allow lower microbial penetration than hypodermic needles in vitro, Pharm. Res. 26 (2009) 2513–2522.
[11] W.Z. Li, M.R. Huo, J.P. Zhou, Y.Q. Zhou, B.H. Hao, T. Liu, Y. Zhang, Super-short solid silicon microneedles for transdermal drug delivery applications, Int. J. Pharm. 389 (2010) 122–129.
[12] H.S. Gill, M.R. Prausnitz, Coated microneedles for transdermal delivery, J. Control. Release 117 (2007) 227–237.
[13] M. Pearton, D. Pirri, S.M. Kang, R.W. Compans, J.C. Birchall, Host responses in human skin after conventional intradermal injection or microneedle administration of virus-like-particle influenza vaccine, Adv. Healthcare Mater. 2 (2013) 1401–1410.
[14] D.G. Koutsonanos, E.V. Vassilieva, A. Stavropoulou, V.G. Zarnitsyn, E.S. Esser, M.T. Taherbhai, M.R. Prausnitz, R.W. Compans, I. Skountzou, Delivery of subunit influenza vaccine to skin with microneedles improves immunogenicity and long-lived protection, Sci. Rep. 2 (2012) 357.
[15] K. van der Maaden, E.M. Varypataki, S. Romeijn, F. Ossendorp, W. Jiskoot, J. Bouwstra, Ovalbumin-coated pH-sensitive microneedle arrays effectively induce ovalbumin-specific antibody and T-cell responses in mice, Eur. J. Pharm. Biopharm. 88 (2014) 310–315.
[16] Y.-C. Kim, J.-M. Song, A.S. Lipatov, S.-O. Choi, J.W. Lee, R.O. Donis, R.W. Compans, S.-M. Kang, M.R. Prausnitz, Increased immunogenicity of avian influenza DNA vaccine delivered to the skin using a microneedle patch, Eur. J. Pharm. Biopharm. 81 (2012) 239–247.
[17] J.B. Carey, F.E. Pearson, A. Vrdoljak, M.G. McGrath, A.M. Crean, P.T. Walsh, T. Doody, C. O'Mahony, A.V. Hill, A.C. Moore, Microneedle array design determines the induction of protective memory CD8+ T cell responses induced by a recombinant live malaria vaccine in mice, PLoS One 6 (2011), e22442.
[18] Y.C. Kim, F.S. Quan, D.G. Yoo, R.W. Compans, S.M. Kang, M.R. Prausnitz, Enhanced memory responses to seasonal H1N1 influenza vaccination of the skin with the use of vaccine-coated microneedles, J. Infect. Dis. 201 (2010) 190–198.
[19] F.S. Quan, Y.C. Kim, R.W. Compans, M.R. Prausnitz, S.M. Kang, Dose sparing enabled by skin immunization with influenza virus-like particle vaccine using microneedles, J. Control. Release 147 (2010) 326–332.
[20] Y. Levin, E. Kochba, R. Kenney, Clinical evaluation of a novel microneedle device for intradermal delivery of an influenza vaccine: are all delivery methods the same? Vaccine 32 (2014) 4249–4252.
[21] A.K. Shakya, H.S. Gill, A comparative study of microneedle-based cutaneous immunization with other conventional routes to assess feasibility of microneedles for allergy immunotherapy, Vaccine 33 (2015) 4060–4064.
[22] N. Romani, B.E. Clausen, P. Stoitzner, Langerhans cells and more: langerin-expressing dendritic cell subsets in the skin, Immunol. Rev. 234 (2010) 120–141.
[23] J. Kerzerho, D. Wunsch, N. Szely, H.A. Meyer, L. Lurz, L. Rose, U. Wahn, O. Akbari, P. Stock, Effects of systemic versus local administration of corticosteroids on mucosal tolerance, J. Immunol. 188 (2011) 470–476.
[24] G. Stary, I. Klein, W. Bauer, F. Koszik, B. Reininger, S. Kohlhofer, K. Gruber, H. Skvara, T. Jung, G. Stingl, Glucocorticosteroids modify Langerhans cells to produce TGF-β and expand regulatory T cells, J. Immunol. 186 (2011) 103–112.
[25] G. Koopman, A.G. Dalgleish, B.S. Bhogal, A.G. Haaksma, J.L. Heeney, Changes in dendritic cell subsets in the lymph nodes of rhesus macaques after application of glucocorticoids, Hum. Immunol. 62 (2001) 208–214.
[26] J. Pan, D. Ju, Q. Wang, M. Zhang, D. Xia, L. Zhang, H. Yu, X. Cao, Dexamethasone inhibits the antigen presentation of dendritic cells in MHC class II pathway, Immunol. Lett. 76 (2001) 153–161.
[27] M. Furue, S.I. Katz, Direct effects of glucocorticosteroids on epidermal Langerhans cells, J. Investig. Dermatol. 92 (1989) 342–347.
[28] D.V. Belsito, T.J. Flotte, H.W. Lim, R.L. Baer, G.J. Thorbecke, I. Gigli, Effect of glucocorticosteroids on epidermal Langerhans cells, J. Exp. Med. 155 (1982) 291–302.
[29] J. Ashworth, J. Booker, S.M. Breathnach, Effects of topical corticosteroid therapy on Langerhans cell antigen presenting function in human skin, Br. J. Dermatol. 118 (1988) 457–469.
[30] S. Grabbe, K. Steinbrink, M. Steinert, T.A. Luger, T. Schwarz, Removal of the majority of epidermal Langerhans cells by topical or systemic steroid application enhances the effector phase of murine contact hypersensitivity, J. Immunol. 155 (1995) 4207–4217.
[31] V. Judkowski, C. Pinilla, K. Schroder, L. Tucker, N. Sarvetnick, D.B. Wilson, Identification of MHC class II-restricted peptide ligands, including a glutamic acid decarboxylase 65 sequence, that stimulate diabetogenic T cells from transgenic BDC2.5 nonobese diabetic mice, J. Immunol. 166 (2001) 908–917.
[32] B.D. Stadinski, T. Delong, N. Reisdorph, R. Reisdorph, R.L. Powell, M. Armstrong, J.D. Piganelli, G. Barbour, B. Bradley, F. Crawford, P. Marrack, S.K. Mahata, J.W. Kappler, K. Haskins, Chromogranin A is an autoantigen in type 1 diabetes, Nat. Immunol. 11 (2010) 225–231.
[33] S. Sasawatari, T. Tadaki, M. Isogai, M. Takahara, M. Nieda, K. Kakimi, Efficient priming and expansion of antigen-specific CD8+ T cells by a novel cell-based artificial APC, Immunol. Cell Biol. 84 (2006) 512–521.
[34] H.S. Gill, M.R. Prausnitz, Coating formulations for microneedles, Pharm. Res. 24 (2007) 1369–1380.
[35] M. Prunieras, M. Regnier, D. Woodley, Methods for cultivation of keratinocytes with an air-liquid interface, J. Invest. Dermatol. 81 (1983) 28s–33s.
[36] R.H. Chong, E. Gonzalez-Gonzalez, M.F. Lara, T.J. Speaker, C.H. Contag, R.L. Kaspar, S.A. Coulman, R. Hargest, J.C. Birchall, Gene silencing following siRNA delivery to skin via coated steel microneedles: in vitro and in vivo proof-of-concept, J. Control. Release 166 (2013) 211–219.
[37] J.S. Kao, J.W. Fluhr, M.-Q. Man, A.J. Fowler, J.-P. Hachem, D. Crumrine, S.K. Ahn, B.E. Brown, P.M. Elias, K.R. Feingold, Short-term glucocorticoid treatment compromises both permeability barrier homeostasis and stratum corneum integrity: inhibition of epidermal lipid synthesis accounts for functional abnormalities, J. Investig. Dermatol. 120 (2003) 456–464.
[38] J. Idoyaga, C. Fiorese, L. Zbytnuik, A. Lubkin, J. Miller, B. Malissen, D. Mucida, M. Merad, R.M. Steinman, Specialized role of migratory dendritic cells in peripheral tolerance induction, J. Clin. Invest. 123 (2013) 844–854.
[39] E. Shklovskaya, B.J. O'Sullivan, L.G. Ng, B. Roediger, R. Thomas, W. Weninger, B. Fazekas de St Groth, Langerhans cells are precommitted to immune tolerance induction, PNAS 108 (2011) 18049–18054.

[40] N. Romani, M. Thurnher, J. Idoyaga, R.M. Steinman, V. Flacher, Targeting of antigens to skin dendritic cells: possibilities to enhance vaccine efficacy, Immunol. Cell Biol. 88 (2010) 424–430.
[41] S. Tamoutounour, M. Guilliams, F. Montanana Sanchis, H. Liu, D. Terhorst, C. Malosse, E. Pollet, L. Ardouin, H. Luche, C. Sanchez, M. Dalod, B. Malissen, S. Henri, Origins and functional specialization of macrophages and of conventional and monocyte-derived dendritic cells in mouse skin, Immunity 39 (2013) 925–938.
[42] T. Rattanapak, J.C. Birchall, K. Young, A. Kubo, S. Fujimori, M. Ishii, S. Hook, Dynamic visualization of dendritic cell-antigen interactions in the skin following transcutaneous immunization, PLoS One 9 (2014), e89503.
[43] G.J. Randolph, V. Angeli, M.A. Swartz, Dendritic-cell trafficking to lymph nodes through lymphatic vessels, Nat. Rev. Immunol. 5 (2005) 617–628.
[44] M. Akbarpour, K.S. Goudy, A. Cantore, F. Russo, F. Sanvito, L. Naldini, A. Annoni, M.G. Roncarolo, Insulin B chain 9–23 gene transfer to hepatocytes protects from type 1 diabetes by inducing Ag-specific FoxP3+ tregs, Sci. Transl. Med. 7 (2015) (289ra281-289ra281).
[45] B.R. Burton, G.J. Britton, H. Fang, J. Verhagen, B. Smithers, C.A. Sabatos-Peyton, L.J. Carney, J. Gough, S. Strobel, D.C. Wraith, Sequential transcriptional changes dictate safe and effective antigen-specific immunotherapy, Nat. Commun. 5 (2014).
[46] J.C. Birchall, R. Clemo, A. Anstey, D.N. John, Microneedles in clinical practice—an exploratory study into the opinions of healthcare professionals and the public, Pharm. Res. 28 (2011) 95–106.
[47] R.J. Dearman, M. Bhushan, M. Cumberbatch, I. Kimber, C.E. Griffiths, Measurement of cytokine expression and Langerhans cell migration in human skin following suction blister formation, Exp. Dermatol. 13 (2004) 452–460.
[48] N. Alexandre, J. Ribeiro, A. Gärtner, T. Pereira, I. Amorim, J. Fragoso, A. Lopes, J. Fernandes, E. Costa, A. Santos-Silva, M. Rodrigues, J.D. Santos, A.C. Maurício, A.L. Luís, Biocompatibility and hemocompatibility of polyvinyl alcohol hydrogel used for vascular grafting—in vitro and in vivo studies, J. Biomed. Mater. Res. A 102 (2014) 4262–4275.
[49] G.B. Ferreira, C.A. Gysemans, J. Demengeot, J.P.M.C.M. da Cunha, A.-S. Vanherwegen, L. Overbergh, T.L. Van Belle, F. Pauwels, A. Verstuyf, H. Korf, C. Mathieu, 1,25-dihydroxyvitamin D3 promotes tolerogenic dendritic cells with functional migratory properties in NOD mice, J. Immunol. 192 (2014) 4210–4220.
[50] P. Van Damme, F. Oosterhuis-Kafeja, M. Van der Wielen, Y. Almagor, O. Sharon, Y. Levin, Safety and efficacy of a novel microneedle device for dose sparing intradermal influenza vaccination in healthy adults, Vaccine 27 (2009) 454–459.
[51] C. Daniel, B. Weigmann, R. Bronson, H. von Boehmer, Prevention of type 1 diabetes in mice by tolerogenic vaccination with a strong agonist insulin mimetope, J. Exp. Med. 208 (2011) 1501–1510.
[52] M. Larche, D.C. Wraith, Peptide-based therapeutic vaccines for allergic and autoimmune diseases, Nat. Med. 11 (2005) S69–S76.
[53] L. Kolbe, A.M. Kligman, V. Schreiner, T. Stoudemayer, Corticosteroid-induced atrophy and barrier impairment measured by non-invasive methods in human skin, Skin Res. Technol. 7 (2001) 73–77.
[54] G. Senti, S. von Moos, T. Kündig, Epicutaneous immunotherapy for aeroallergen and food allergy, Curr. Treat Options Allergy 1 (2014) 68–78.
[55] C.A. Akdis, M. Akdis, Advances in allergen immunotherapy: aiming for complete tolerance to allergens, Sci. Transl. Med. 7 (2015) (280ps286-280ps286.).
[56] M. Szczepanik, M. Tutaj, K. Bryniarski, B.N. Dittel, Epicutaneously induced TGF-beta-dependent tolerance inhibits experimental autoimmune encephalomyelitis, J. Neuroimmunol. 164 (2005) 105–114.
[57] M.S. Bynoe, J.T. Evans, C. Viret, C.A. Janeway, Epicutaneous immunization with autoantigenic peptides induces T suppressor cells that prevent experimental allergic encephalomyelitis, Immunity 19 (2003) 317–328.
[58] C. Dupont, N. Kalach, P. Soulaines, S. Legoue-Morillon, H. Piloquet, P.H. Benhamou, Cow's milk epicutaneous immunotherapy in children: a pilot trial of safety, acceptability, and impact on allergic reactivity, J. Allergy Clin. Immunol. 125 (2010) 1165–1167.
[59] G. Senti, S. von Moos, T.M. Kundig, Epicutaneous allergen administration: is this the future of allergen-specific immunotherapy? Allergy 66 (2011) 798–809.
[60] G. Senti, S. von Moos, F. Tay, N. Graf, P. Johansen, T.M. Kundig, Determinants of efficacy and safety in epicutaneous allergen immunotherapy: summary of three clinical trials, Allergy 70 (2015) 707–710.
[61] J. Strid, J. Hourihane, I. Kimber, R. Callard, S. Strobel, Epicutaneous exposure to peanut protein prevents oral tolerance and enhances allergic sensitization, Clin. Exp. Allergy 35 (2005) 757–766.
[62] P.A. Gottlieb, T. Delong, R.L. Baker, L. Fitzgerald-Miller, R. Wagner, G. Cook, M.R. Rewers, A. Michels, K. Haskins, Chromogranin A is a T cell antigen in human type 1 diabetes, J. Autoimmun. 50 (2014) 38–41.
[63] D. Daniel, D.R. Wegmann, Protection of nonobese diabetic mice from diabetes by intranasal or subcutaneous administration of insulin peptide B-(9–23), PNAS 93 (1996) 956–960.
[64] D.G. Alleva, P.D. Crowe, L. Jin, W.W. Kwok, N. Ling, M. Gottschalk, P.J. Conlon, P.A. Gottlieb, A.L. Putnam, A. Gaur, A disease-associated cellular immune response in type 1 diabetics to an immunodominant epitope of insulin, J. Clin. Invest. 107 (2001) 173–180.
[65] K. Nakayama, H. Matsuura, M. Asai, K.-i. Ogawara, K. Higaki, T. Kimura, Estimation of intradermal disposition kinetics of drugs: I. Analysis by compartment model with contralateral tissues, Pharm. Res. 16 (1999) 302–308.
[66] V.B. Gibson, T. Nikolic, V.Q. Pearce, O. Demengeot, B.O. Roep, M. Peakman, Proinsulin multi-peptide immunotherapy induces antigen-specific regulatory T cells and limits autoimmunity in a humanised model, Clin. Exp. Immunol. 182 (2015) 251–260.
[67] H.B. Streeter, R. Rigden, K.F. Martin, N.J. Scolding, D.C. Wraith, Preclinical development and first-in-human study of ATX-MS-1467 for immunotherapy of MS, Neurol. Neuroimmunol. Neuroinflamm. 2 (2015), e93.
[68] E.Z. Giannopoulou, C. Winkler, R. Chmiel, C. Matzke, M. Scholz, A. Beyerlein, P. Achenbach, E. Bonifacio, A.G. Ziegler, Islet autoantibody phenotypes and incidence in children at increased risk for type 1 diabetes, Diabetologia 58 (2015) 2317–2323.
[69] J.M. Sosenko, J.S. Skyler, L.A. DiMeglio, C.A. Beam, J.P. Krischer, C.J. Greenbaum, D. Boulware, L.E. Rafkin, D. Matheson, K.C. Herold, J. Mahon, J.P. Palmer, T.D.T.S. Group, D.P.T.-T.S. Group, A new approach for diagnosing type 1 diabetes in autoantibody-positive individuals based on prediction and natural history, Diabetes Care 38 (2015) 271–276.